Singular value decomposition and 2D crosscorrelation based localization of gas vesicles for super-resolution ultrasound imaging

Jihun Kim
Aerospace and Mechanical
Engineering
University of Notre Dame
Notre Dame, IN, USA
jkim75@nd.edu

Gyoyeon Hwang
Aerospace and Mechanical
Engineering
University of Notre Dame
Notre Dame, IN, USA
ghwang@nd.edu

Sunghoon Rho
Aerospace and Mechanical
Engineering
University of Notre Dame
Notre Dame, IN, USA
srho@nd.edu

Sangpil Yoon
Aerospace and Mechanical
Engineering
University of Notre Dame
Notre Dame, IN, USA
syoon4@nd.edu

Abstract—We report the potentials of nanometer-sized contrast agents which are called gas vesicles (GVs) for super-resolution ultrasound (SRUS) imaging to diagnose of vasculature deep inside tissue. Thus, we developed the GVs and ultrasound localization microscopy (ULM) based on singular value decomposition and 2D cross-correlation techniques. Furthermore, the SRUS imaging of the vessel-mimicking phantom with the GVs was performed. These results demonstrate that GVs could have potentials as novel contrast agents at nanoscale for implementing the SRUS imaging, thus indicating that ULM with GVs would be used for better visualization of micro-vasculature in vivo.

Keywords—Super-resolution ultrasound imaging, Contrast agent, Gas vesicles, Nanoscale acoustic biomolecules

I. Introduction (Heading 1)

For clinical diagnosis and biological research using ultrasound imaging, the microbubbles (MBs) have been introduced as the contrast agents (CAs) to enhance the contrast of the ultrasound image. Besides, MBs have been utilized for blood-brain barrier opening and drug/gene delivery by the bubble cavitation-induced permeability improvement of vessel and cell membranes [1-3]. In recent, MBs has been utilized for super-resolution ultrasound (SRUS) imaging based on localization of MBs centroid by normalized 2D cross-correlation (2D-CC) to examine the structural and dysfunction of the vessel in liver, kidney, brain, as well as the tumor by localization of MBs through the bloodstream beyond the diffraction limit of conventional ultrasound imaging conserving the imaging depth [4-9]. To remove the clutter signals in ultrasound imaging before localization, singular value decomposition (SVD) filtering was demonstrated as a suitable processing step before localizing MBs, which offers

This work was supported in part by National Institute of Health (NIH) grant No. GM120493, National Science Foundation (NSF) grant No. 1943852, 2019 AD&T Discovery Fund, and Walther Cancer Foundation Advancing Basic Cancer grants.

precise localization of MBs in the range of few micrometers [10].

MBs that have the diameter of several micrometers and consist of gas-cored and shell of lipid, polymer, or albumin is restricted mainly use for blood vessels owing to relatively large size (e.g. 1 – 8 μm in diameter) [11]. In recent, gas vesicles (GVs), which are gas-filled protein-shelled nanostructures, has been introduced as a new class of nanoscale bubbles for an ultrasound and magnetic resonance imaging [12]. The GVs generally has the size ranging from 45-200 nm in width 100-800 nm in length and depending on the organism. It also can provide the longer sustainability in circulation. Besides, GVs could be genetically engineered for multimodal imaging qualitatively [13]. Thus, we developed the nanoscale GVs in order to examine the potentials for the reconstruction of the SR-US image, which would provide the longer retention time in circulation and support to visualize the extra-vascular space of cancerous tissue beyond the endothelial cells layer which could not be accessed by traditional MBs [14].

In this paper, we examine the potentials of SRUS imaging technique with the nanoscale acoustic contrast agents, called GVs, for visualization of vasculature. For an evaluation of the proposed technique, uniformly distributed point targets (PTs) were generated and localized in ultrasound simulation. Furthermore, we carried out the SRUS imaging of vesselminicking phantom using the GVs.

II. MATERIALS AND METHODS

A. Preparation of nanoscale gas vesicles

GVs were purified from Bacillus megaterium (Mega) [15]. GV concentration was determined by optical density at 500 nm (OD₅₀₀) using a Nanodrop 2000 spectrophotometer (ThermoFisher, Waltham, MA). Figs. 1(a) and 1(b) show the

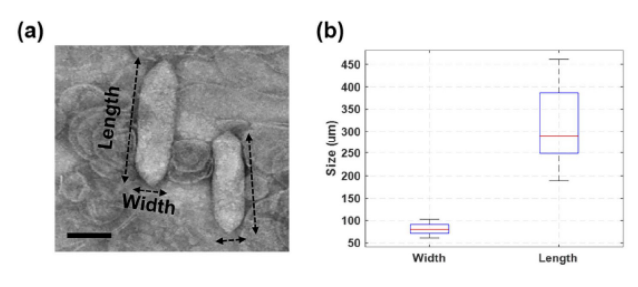


Fig. 1. Nanoscale megaterium gas vesicles: (a) A transmission electron microscope image of gas vesicles, (b) Size distribution in width and length respectively. The measured mean with the standard deviation of width and length are 80 ± 12.2 nm and 312 ± 81.2 nm, respectively.

transmission electron microscope image and measured size of Mega GVs we developed. The measured mean with the standard deviation of width and length are 80 ± 12.2 nm and 312 ± 81.2 nm, respectively

B. Preparation of point targets in simulation and vesselmimicking phantom

For evaluation of the localization technique, normalized 2D-CC algorithm, the uniformly distributed PTs in simulation were generated. First, the uniformly distributed nine-PTs were constructed at each inter-points distance D from 0.5 to 2.5 λ with a step size of 0.5 λ in axial and lateral directions. The λ is correspondent with 55 μ m.

After the evaluation of the localization technique in ultrasound simulation, we performed the SR-US imaging of a vessel-mimicking phantom by flowing the Mega GVs through the vessel. First, the agar powder (1%), and 10 μm diameter silica powders (2%) were mixed in deionized (100 g) water by heating [16]. To establish the wall-less vessel inside the phantom, the glass rod with 500 μm diameter was lied between inlet and outlet at the chamber at a 15 degree. Then, the glass rod was removed after confirming that it was solidified. The Mega GVs with OD500 of 20 were flowed at a volume rate of 100 $\mu L/min$ through the vessel.

C. Super-resolution ultrasound imaging technique

We used an ultrasound imaging system (Vantage 256, Verasonics Inc., USA) with a high-frequency linear array transducer (L35-16vx. Verasonics Inc., USA) by

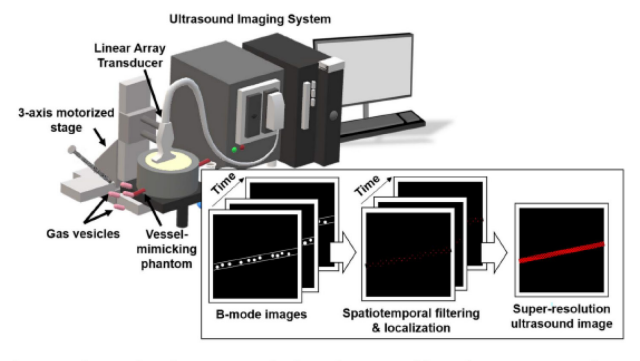


Fig. 2. Schematic of super-resolution ultrasound imaging system and postprocessing procedure for reconstruction of super-resolution ultrasound image of vessel with GVs.

incorporating the transducer to the 3-axis motorized stage (ILS150CC, Newport Inc., USA) as shown in Fig 2. A five angle (-7° to 7°) plane-wave compounding with an effective pulse repetition frequency of 100 Hz and the transmit frequency of 25 MHz was used. A total of 500 compounded IO data sets were acquired.

To detect the GVs signals in the vessel, we first removed the clutter signals by applying the spatiotemporal filter using SVD [17]. The normalized 2D-CC was then conducted between the 4 times spatially interpolated GVs and PSF signals. The cross-correlation coefficient map was thresholded with the value of 0.6 and then identified the each centroid of GVs by applying the regional maximum identification algorithm ('imregionalmax.m' in Matlab) to identified the centroid of each GVs at each frame. Subsequently, the SRUS image was reconstructed by superposing the localization results of GVs at each frame.

III. RESULTS AND DISCUSSION

A. Evaluation of localization technique in simulation

We first analyze the limitation of the localization technique for normalized 2D-CC using the uniformly distributed PTs in simulation. Figs. 2(a) and 2(b) show the localization results overlaid on the conventional B-mode image of uniformly distributed PTs with the spacing of 2λ and 2.5λ . For 2.5λ spacing, every PTs were localized while six PTs were identified for 2λ spacing. In addition, the lower performance for localization was represented for laterally distributed PTs than in axially distributed PTs. Further, we measured the detection rate depending on the spacing. Detection rate was calculated by dividing the number of localized points by the simulated number of points. As shown in Fig. 3(c), the detection rate was confirmed under 50 % under the 1.5λ spacing.

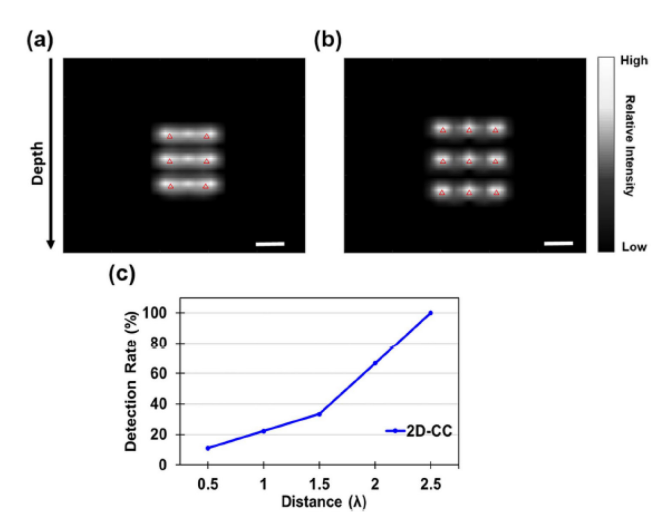


Fig. 3. Evaluation of localization technique using uniformly distributed nine-point targets in simulation: Localized results overlaid on B-mode image of point targets with (a) 2 λ and (b) 2.5 λ spacing, respectively. Red triangles show the localized points using 2D cross-correlation. The scale bars represent the 100 μ m. (c) Detection rate depending on the spacing between points. The λ is correspondent with 55 μ m.

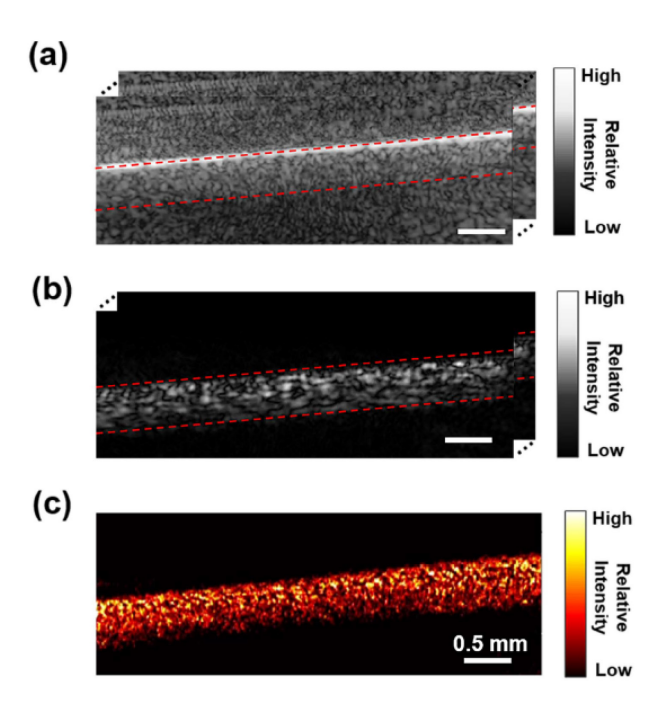


Fig. 4. Reconstruction of super-resolution ultrasound image of vessel-mimicking phantom with megaterium gas vesicles: (a) Time sequence B-mode images of vessel-mimicking phantom, (b) Clutter filtering by singular value decomposition, (c) Super-resolution ultrasound image of microvasculature.

B. Super-resolution ultrasound imaging of vesselmimicking phantom

After the evaluation of the normalized 2D-CC for localization using the uniformly distributed PTs in simulation, we carried out the SRUS imaging of vessel-mimicking phantom with the Mega GVs. Figs. 4(a) and 4(b) represent the acquired B-mode and SVD filtered image of vessel-mimicking phantom. Then, we reconstructed the SR-US image of vasculature obtained by normalized 2D-CC. This image was reconstructed by accumulating the localization results of 500 frames. The micro-vasculature in the phantom was visualized with Mega GVs by applying the SVD and 2D-CC techniques [Fig. 4(c)].

Altogether, these results demonstrate that SVD and 2D-CC based localization approach can be used for super-resolution ultrasound imaging to visualize microvasculature

IV. CONCLUSIONS

In conclusion, we demonstrated the SRUS imaging of microvasculature with nanoscale acoustic molecules. The potentials of GVs as the CAs for the reconstruction of the SRUS image was validated. In the future, we will carry out the SRUS imaging of the vasculature of zebrafish *in vivo* to further demonstrate the capability of SRUS imaging with different types of GVs.

REFERENCES

[1] N. A. Geis, H. A. Katus, and R. Bekeredjian, "Microbubbles as a vehicle for gene and drug delivery: current clinical implications and future

- perspectives," *Current pharmaceutical design*, vol. 18, no. 15, pp. 2166-2183, 2012.
- [2] C.-Y. Ting *et al.*, "Concurrent blood–brain barrier opening and local drug delivery using drug-carrying microbubbles and focused ultrasound for brain glioma treatment," *Biomaterials*, vol. 33, no. 2, pp. 704-712, 2012.
- [3] F. Yan *et al.*, "Paclitaxel-liposome–microbubble complexes as ultrasound-triggered therapeutic drug delivery carriers," *Journal of controlled release*, vol. 166, no. 3, pp. 246-255, 2013.
- [4] K. Christensen-Jeffries, R. J. Browning, M.-X. Tang, C. Dunsby, and R. J. Eckersley, "In vivo acoustic super-resolution and super-resolved velocity mapping using microbubbles," *IEEE* transactions on medical imaging, vol. 34, no. 2, pp. 433-440, 2014.
- [5] J. Foiret, H. Zhang, T. Ilovitsh, L. Mahakian, S. Tam, and K. W. Ferrara, "Ultrasound localization microscopy to image and assess microvasculature in a rat kidney," *Scientific reports*, vol. 7, no. 1, p. 13662, 2017.
- [6] P. Song et al., "Improved Super-Resolution Ultrasound Microvessel Imaging With Spatiotemporal Nonlocal Means Filtering and Bipartite Graph-Based Microbubble Tracking," IEEE Trans Ultrason Ferroelectr Freq Control, vol. 65, no. 2, pp. 149-167, Feb 2018, doi: 10.1109/TUFFC.2017.2778941.
- [7] C. Errico et al., "Ultrafast ultrasound localization microscopy for deep super-resolution vascular imaging," *Nature*, vol. 527, no. 7579, pp. 499-502, 2015.
- [8] F. Lin, S. E. Shelton, D. Espíndola, J. D. Rojas, G. Pinton, and P. A. Dayton, "3-D ultrasound localization microscopy for identifying microvascular morphology features of tumor angiogenesis at a resolution beyond the diffraction limit of conventional ultrasound," *Theranostics*, vol. 7, no. 1, p. 196, 2017.
- [9] J. Yu, L. Lavery, and K. Kim, "Super-resolution ultrasound imaging method for microvasculature in vivo with a high temporal accuracy," *Scientific reports*, vol. 8, no. 1, pp. 1-11, 2018.
- [10] J. Brown *et al.*, "Investigation of microbubble detection methods for super-resolution imaging of microvasculature," *IEEE transactions on ultrasonics, ferroelectrics, and frequency control*, vol. 66, no. 4, pp. 676-691, 2019.
- [11] N. De Jong, M. Emmer, A. Van Wamel, and M. Versluis, "Ultrasonic characterization of ultrasound contrast agents," *Medical & biological engineering & computing*, vol. 47, no. 8, pp. 861-873, 2009.
- [12] M. G. Shapiro *et al.*, "Biogenic gas nanostructures as ultrasonic molecular reporters," *Nature nanotechnology*, vol. 9, no. 4, p. 311, 2014.

- [13] A. Lakshmanan *et al.*, "Molecular engineering of acoustic protein nanostructures," *ACS nano*, vol. 10, no. 8, pp. 7314-7322, 2016.
- [14] S. A. Peyman *et al.*, "On-chip preparation of nanoscale contrast agents towards high-resolution ultrasound imaging," *Lab on a Chip*, vol. 16, no. 4, pp. 679-687, 2016.
- [15] A. Lakshmanan *et al.*, "Preparation of biogenic gas vesicle nanostructures for use as contrast agents for ultrasound and MRI," *Nature protocols*, vol. 12, no. 10, p. 2050, 2017.
- [16] X. Zhou, D. A. Kenwright, S. Wang, J. A. Hossack, and P. R. Hoskins, "Fabrication of Two Flow Phantoms for Doppler Ultrasound Imaging," *IEEE Trans Ultrason Ferroelectr Freq Control*, vol. 64, no. 1, pp. 53-65, Jan 2017, doi: 10.1109/TUFFC.2016.2634919.
- [17] C. Demene *et al.*, "Spatiotemporal Clutter Filtering of Ultrafast Ultrasound Data Highly Increases Doppler and fUltrasound Sensitivity," *IEEE Trans Med Imaging*, vol. 34, no. 11, pp. 2271-85, Nov 2015, doi: 10.1109/TMI.2015.2428634.